

Accepted for Publication in the Astronomical Journal

The ALFALFA “Almost Darks” Campaign: Pilot VLA HI Observations of Five High Mass-to-Light Ratio Systems

John M. Cannon

*Department of Physics & Astronomy, Macalester College, 1600 Grand Avenue, Saint Paul,
MN 55105*

`jcannon@macalester.edu`

Charlotte P. Martinkus

*Department of Physics & Astronomy, Macalester College, 1600 Grand Avenue, Saint Paul,
MN 55105*

`cmartink@macalester.edu`

Lukas Leisman

*Center for Radiophysics and Space Research, Space Sciences Building, Cornell University,
Ithaca, NY 14853, USA*

`leisman@astro.cornell.edu`

Martha P. Haynes

*Center for Radiophysics and Space Research, Space Sciences Building, Cornell University,
Ithaca, NY 14853, USA*

`haynes@astro.cornell.edu`

Elizabeth A. K. Adams

*Netherlands Institute for Radio Astronomy (ASTRON), Postbus 2, 7990 AA, Dwingeloo,
The Netherlands*

`adams@astron.nl`

Riccardo Giovanelli

*Center for Radiophysics and Space Research, Space Sciences Building, Cornell University,
Ithaca, NY 14853, USA*

`riccardo@astro.cornell.edu`

Gregory Hallenbeck

*Center for Radiophysics and Space Research, Space Sciences Building, Cornell University,
Ithaca, NY 14853, USA*

Department of Physics and Astronomy, Union College, Schenectady, NY 12308, USA

`hallenbg@union.edu`

Steven Janowiecki

*Department of Astronomy, Indiana University, 727 East Third Street, Bloomington, IN
47405, USA*

`sjanowie@indiana.edu`

Michael Jones

*Center for Radiophysics and Space Research, Space Sciences Building, Cornell University,
Ithaca, NY 14853, USA*

`jonesmg@astro.cornell.edu`

Gyula I.G. Józsa

*SKA South Africa, Radio Astronomy Research Group, 3rd Floor, The Park, Park Road,
Pinelands, 7405, South Africa*

*Rhodes University, Department of Physics and Electronics, Rhodes Centre for Radio
Astronomy Techniques & Technologies, PO Box 94, Grahamstown, 6140, South Africa*

Argelander-Institut für Astronomie, Auf dem Hügel 71, 53121 Bonn, Germany

`jozsa@ska.ac.za`

Rebecca A. Koopmann

Department of Physics and Astronomy, Union College, Schenectady, NY 12308, USA

`koopmanr@union.edu`

Nathan Nichols

Hartwick College, Oneonta, NY 13820, USA

nicholsn@hartwick.edu

Emmanouil Papastergis

*Kapteyn Astronomical Institute, University of Groningen, Postbus 800, 9700 AA,
Groningen, The Netherlands*

papastergis@astro.rug.nl

Katherine L. Rhode

*Department of Astronomy, Indiana University, 727 East Third Street, Bloomington, IN
47405, USA*

rhode@astro.indiana.edu,

John J. Salzer

*Department of Astronomy, Indiana University, 727 East Third Street, Bloomington, IN
47405, USA*

slaz@astro.indiana.edu

Parker Troischt

Hartwick College, Oneonta, NY 13820, USA

troischt@hartwick.edu

ABSTRACT

We present new VLA H I spectral line imaging of five sources discovered by the ALFALFA extragalactic survey. These targets are drawn from a larger sample of systems that were not uniquely identified with optical counterparts during ALFALFA processing, and as such have unusually high H I mass to light ratios. The candidate “Almost Dark” objects fall into four broad categories: 1) objects with nearby H I neighbors that are likely of tidal origin; 2) objects that appear to be part of a system of multiple H I sources, but which may not be tidal in origin; 3) objects isolated from nearby ALFALFA H I detections, but located near a gas-poor early-type galaxy; 4) apparently isolated sources, with no object of coincident redshift within ~ 400 kpc. Roughly 75% of the 200 objects without identified counterparts in the $\alpha.40$ database (Haynes et al. 2011) fall into

category 1 (likely tidal), and were not considered for synthesis follow-up observations. The pilot sample presented here (AGC 193953, AGC 208602, AGC 208399, AGC 226178, and AGC 233638) contains the first five sources observed as part of a larger effort to characterize H I sources with no readily identifiable optical counterpart at single dish resolution ($3.5'$). These objects span a range of H I mass [$7.41 < \log(M_{\text{HI}}) < 9.51$] and H I mass to B-band luminosity ratios ($3 < M_{\text{HI}}/L_{\text{B}} < 9$). We compare the H I total intensity and velocity fields to optical imaging drawn from the Sloan Digital Sky Survey and to ultraviolet imaging drawn from archival GALEX observations. Four of the sources with uncertain or no optical counterpart in the ALFALFA data are identified with low surface brightness optical counterparts in Sloan Digital Sky Survey imaging when compared with VLA H I intensity maps, and appear to be galaxies with clear signs of ordered rotation in the H I velocity fields. Three of these are detected in far-ultraviolet GALEX images, a likely indication of star formation within the last few hundred Myrs. One source (AGC 208602) is likely tidal in nature, associated with the NGC 3370 group. Consistent with previous efforts, we find no “dark galaxies” in this limited sample. However, the present observations do reveal complex sources with suppressed star formation, highlighting both the observational difficulties and the necessity of synthesis follow-up observations to understand these extreme objects.

Subject headings: galaxies: evolution — galaxies: dwarf — galaxies: irregular — galaxies: individual (AGC193953, AGC208602, AGC208399, AGC226178, AGC233638)

1. Introduction

ALFALFA, the Arecibo Legacy Fast ALFA extragalactic H I survey, has obtained a census of H I-bearing galaxies over 7000 square degrees of high Galactic latitude sky visible from Arecibo between $0^\circ < \delta < +36^\circ$ (Giovanelli et al. 2005; Haynes et al. 2011). Its combination of sensitivity, bandwidth and sky coverage make ALFALFA the first wide area H I survey to sample a cosmologically significant volume, delivering robust determinations of the H I mass, width, and diameter functions, the H I correlation function, and the cosmic density of H I at $z \sim 0$ (Martin et al. 2010; Dowell et al. 2011; Papastergis et al. 2011; Martin et al. 2012). When completed, the final ALFALFA database will contain more than 30,000 high S/N H I detections.

As discussed in Haynes et al. (2011), the 40% ALFALFA catalog (hereafter “ $\alpha.40$ ”) con-

tains 15,855 extragalactic H I sources. Less than 1.5% of these sources were not clearly identified with an associated stellar population (hereafter referred to as an “optical counterpart”) in an optical survey (SDSS or DSS). Of these, only ~ 50 were not readily associated with a known structure or nearby H I source (that is, roughly 75% of these “dark” candidates are likely tidal in origin). The nature of the remaining objects remains unclear; their optical associations are often ambiguous given the ALFALFA pointing accuracy ($\sim 26''$ for reasonable S/N sources) and unresolved given the ALFALFA beam ($3.5'$). As discussed in detail below, there are only a few viable candidate “dark” galaxies in the current literature; the rich population of sources measured by ALFALFA is a promising place to look for more.

To probe the nature of these candidate “dark” objects, we have initiated the ALFALFA “Almost Darks” program: a comprehensive, multi-wavelength follow-up observing campaign to characterize the nature of ALFALFA H I detections that were not identified with an unambiguous optical counterpart in initial ALFALFA processing. We anticipate that detailed studies of these objects will result in the confirmation of associated optical counterparts for the vast majority of systems. Figure 1 shows these objects in comparison to the full $\alpha.40$ catalog; the 11,300 ALFALFA sources with good SDSS photometry (see Haynes et al. 2011) are plotted as either individual black points, or as colored contours at 10% levels (between 10% and 90%) of the number density of sources. Optical luminosities for these sources are calculated using SDSS catalog magnitudes from the ALFALFA-SDSS cross match presented in Haynes et al. (2011). The 52 candidate “dark” sources are shown in red, with the 5 objects selected for the pilot sample studied in detail in the present manuscript shown in green. These 52 sources are those that have no clear optical counterpart assigned in the initial ALFALFA processing, and that were not deemed as likely to be tidal in nature. Red points represent upper limits in luminosity estimated at the limiting magnitude for a source $10''$ in diameter in downloaded SDSS images. Green points that are not upper limits are calculated using the SDSS catalog magnitudes of the optical counterparts identified after VLA observations; prior to source localization with the VLA these objects were upper limits similar to the points plotted in red.

While Figure 1 was not used for the selection of candidate “Almost Dark” sources, it does clearly demonstrate that these systems harbor high H I mass to stellar light ratios (hereafter, M_{HI}/L) compared to the vast majority of $\alpha.40$ detections. Note that some sources with elevated M_{HI}/L ratios are not classified as candidate “Almost Dark” systems: these sources have clearly associated optical counterparts. Further, while no strict minimum value of M_{HI}/L was enforced to create the sample of “Almost Dark” systems, an empirical threshold (which does have significant uncertainty at low luminosity and low surface brightness) appears around $M_{\text{HI}}/L \simeq 10$.

In this manuscript we present pilot VLA H I spectral line observations of 5 candidate “Almost Dark” sources. This represents the first step in a major program to understand the nature and origin of the most extreme M_{HI}/L systems within the context of various scenarios for their existence: as tidal features, as galaxies with extremely low surface brightness stellar populations, or as genuine “dark” galaxies. The ALFALFA “Almost Dark” objects fall into four broad categories: 1) objects with nearby H I neighbors that are likely of tidal origin; 2) objects that appear to be part of a system of multiple H I sources, but which may not be tidal in origin; 3) objects isolated from nearby ALFALFA H I detections, but located near a gas-poor early-type galaxy; 4) apparently isolated sources, with no object of coincident redshift within ~ 400 kpc. The five sources presented here (AGC 193953, AGC 208602, AGC 208399, AGC 226178, and AGC 233638) populate each of the last three categories (sources with a clear tidal origin from ALFALFA data products were not targeted for interferometric follow-up). Table 1 summarizes the basic properties of the five sources, including position, distance, and H I properties (derived from ALFALFA measurements). This limited sample is not meant to be representative of the “Almost Dark” galaxy sample as a whole; these specific sources were selected in part to fit into pre-approved LST observing slots for VLA scheduling (see § 2.1).

There has been widespread interest in identifying truly “dark” galaxies, if they exist. With the advent of sensitive, wide-area H I surveys such as ALFALFA, and with the increased availability of mapping observations of nearby groups with single dish telescopes, a number of candidate “dark galaxies” have appeared in the literature. These are systems whose H I properties are representative of galaxies, but that lack a clear optical counterpart. The VIRGO HI 21 cloud was originally postulated to be a true dark galaxy (Minchin et al. 2005, 2007). However, subsequent observations (Haynes et al. 2007) and modeling (Duc & Bournaud 2008) have shown that this source is likely tidal in nature. More recently, single-dish telescopes have been used in mapping mode to produce deep targeted H I images of nearby groups. In such a survey of the M 101 group, Mihos et al. (2012) discovered a gas cloud labeled as GBT 1355+5439. In that same work, very deep ground-based optical imaging revealed no obvious stellar counterpart to a limiting surface brightness of $\mu_V = 29$ mag arcsec $^{-2}$. Subsequent interferometric H I observations by Oosterloo et al. (2013) confirm the extreme characteristics of GBT 1355+5439; both a tidal interpretation and an interpretation as a truly “dark” object remain viable. Numerous other sources are interesting and relevant in this context (see discussion and references in Walter et al. 2005, Kent et al. 2009, English et al. 2010, Kent 2010, Matsuoka et al. 2012, Serra et al. 2013, Lee-Waddell et al. 2014, Adams et al. 2014).

We organize this manuscript as follows. In § 2 we discuss the details of the H I data reductions and image production, as well as the techniques applied to derive optical and

ultraviolet (UV) properties from SDSS and GALEX images. § 3 presents the H I, optical, and UV images of each of the five sources; using these data, we can localize the H I gas with confidence, assign possible optical counterparts (by comparison with optical imaging), and search for ordered motions that are indicative of galaxy-like rotation. In § 4 we further discuss the five “Almost Dark” sources in the context of the ALFALFA database, the low-mass galaxies within it, and also among the (growing) list of “Almost Dark” candidates. We draw our conclusions in § 5; primary among these is that none of the five candidate objects appears to qualify as a bona fide “dark galaxy”.

2. Observations and Data Handling

2.1. HI Observations

H I spectral line imaging of the five sources presented in this work was obtained with the National Radio Astronomy Observatory’s *Karl G. Jansky Very Large Array* (VLA¹) in April, 2013, for program 13A-028 (legacy ID AC1116; P.I. Cannon). The five sources selected for observing were the best fits based on the LST oversubscription of the VLA during the 13A semester. The observations were acquired during four separate two-hour observation blocks and during one 2.5-hour block (for source AGC 193953) with the observatory in the “D” (most compact) configuration. The WIDAR correlator was used to divide an 8 MHz bandwidth into 1024 channels. The resulting channel separation of 7.812 kHz ch^{−1} delivers a native spectral resolution of 1.65 km s^{−1} ch^{−1} at the rest frequency of the H I spectral line. Reductions followed standard prescriptions and used both the Astronomical Image Processing System (AIPS) and the Common Astronomy Software Applications (CASA) packages.

Radio frequency interference (RFI) and bad data were removed manually from each dataset. The RFI contamination of the AGC 193953 dataset was significant in a few channels close to those containing the source; the loss of sensitivity in these channels has affected our recovery of flux from this source (see further discussion below). Bandpass and flux calibrations used the standard calibrator 3C286 for all five observing blocks. For each source, a nearby quasar was observed every ∼20 minutes and used to calibrate the phases. We estimate our absolute flux calibration to be accurate at the ∼10% level.

The imaging of the calibrated *uv* databases followed standard prescriptions. To increase S/N, each database was spectrally averaged by a factor of two, to produce a velocity reso-

¹The National Radio Astronomy Observatory is a facility of the National Science Foundation operated under cooperative agreement by Associated Universities, Inc.

lution of $15.625 \text{ kHz ch}^{-1}$ ($3.3 \text{ km s}^{-1} \text{ ch}^{-1}$) prior to imaging. Each cube was inverted with minimal cleaning, and source(s) were identified. Using these full cubes, regions were identified that excluded H I line sources and bandpass edge effects. Using these regions (typically 50 channels or more, depending on the complexity of emission within each cube) as fitting points, the continuum was then subtracted in the uv plane using a first-order polynomial function.

The final spectral line cubes used in this analysis were produced using the IMAGR task in AIPS, with a weighting ROBUST factor of 0.5. Using clean boxes that tightly encompass the high S/N line emission, each cube was deeply cleaned to one half of the RMS level found in line-free channels. Residual flux rescaling was enforced during the imaging process (Jorsater & van Moorsel 1995). The moment zero maps shown below were produced following the THINGS procedures as described in Walter et al. (2008). The original-resolution cubes were convolved to the nearest integer circular sizes in arcseconds (so, for example, the $48.97'' \times 43.00''$ cube for AGC 208602 was convolved to a circular beam size of $49''$) and were then used for all subsequent analyses. A second convolution was enacted to produce cubes with circular beam sizes $\sim 10\%$ larger; these smoothed cubes were blanked at the 2.5σ level, closely examined by eye to retain only emission that is coherent in velocity space, and then used as masks against the original (circular beam size) cubes. Moment zero maps (representing total H I emission) were produced by collapsing these masked cubes. The resulting images of each source are discussed in detail below. The total H I flux integral for each of the five sources is less than the flux integral derived from the ALFALFA observations; we discuss the recovered flux from each source in the sections that follow.

The velocity structure of the H I gas in each source plays an important role in the interpretation of these data; the presence of ordered gas motion is very strong evidence for classifying a candidate “Almost Dark” source as a bona-fide galaxy. As discussed in detail for each individual system below, whenever possible we have used Gaussian fitting to the full (unblanked) datacubes in order to extract the velocity fields of the “Almost Dark” systems presented below. Specifically, we use the GIPSY task XGAUFIT to fit Gaussian functions to emission above the 3σ level in regions of each datacube immediately surrounding 4 of the 5 “Almost Dark” sources; these Gaussian-fitted velocity fields are shown in the 4-panel images presented in § 3. For AGC 208602, the incoherent velocity structure of the source precluded meaningful Gaussian fitting. For those “Almost Dark” sources that have neighboring H I-rich galaxies that are detected in the datacubes (AGC 208602, AGC 226178, and AGC 233638), we also show full-field images including all detected galaxies using the more traditional moment one approach (i.e., collapsing of the blanked data cube) for creating the velocity fields.

2.2. Optical Observations

To quantify the optical properties of these five “Almost Dark” sources, we extract photometry from the Sloan Digital Sky Survey 10th data release products (Ahn et al. 2014). Mosaic frames in the SDSS-g and the SDSS-r bands, using primary covering fields, were created using the SDSS online interface. Integrated magnitudes were derived for each of the “Almost Dark” sources using the LAMBDAAR source extraction code (Wright et al., in preparation²). Elliptical apertures, centered on the H I centroid positions (see Table 1) and with semi-major and semi-minor axis lengths as shown in Table 2, were used to extract the SDSS-g magnitudes and (g–r) colors of each source. The aperture sizes and orientations were set by hand in order to enclose all of the optical flux from each source when the SDSS images were displayed at the highest contrast levels.

The photometry in Table 2 is used to derive the physical parameters of the five “Almost Dark” sources shown in Table 3. After correcting for foreground Galactic absorption (Schlafly & Finkbeiner 2011), the SDSS g magnitude is converted to a Johnson-Cousins B magnitude via the prescriptions in Table 2 of Blanton & Roweis (2007). These (absorption corrected) apparent magnitudes are converted to absolute magnitudes using our assumed distances from Table 1, and then converted to solar luminosities using the values from Table 1 of Blanton & Roweis (2007). The resulting g and B-band luminosities of each “Almost Dark” source are tabulated and compared with the total H I masses (using the ALFALFA flux integrals) in Table 3. This table reveals that the M_{HI}/L ratios span more than a factor of 10 across this small sample. It is important to stress that all of our measurements of the optical properties of these sources are brighter than the pipeline SDSS values; this is a result of the more careful aperture placement and background subtraction done here than by the standard SDSS pipeline measuring tools.

We use the measured r-band magnitude, (g–r) color, and the relations from Zibetti et al. (2009) to derive the stellar mass and M_{HI}/M_{\star} ratio of each candidate “Almost Dark” source shown in Table 3. We stress that these representative stellar masses are uncertain at the $\sim 50\%$ level due to systematic uncertainties alone. Nonetheless, these values can be compared to those for the full $\alpha.40$ catalog using the same technique; we explore this comparison later in this manuscript.

A detailed investigation of the optical properties of the ALFALFA “Almost Darks” sam-

²For details see <https://github.com/AngusWright/LAMBDAAR>

ple is currently underway with the One Degree Imager (ODI³) on the WIYN 3.5m telescope⁴. The results of this endeavor will be presented in a forthcoming manuscript (Janowiecki et al., in preparation). As of this writing, preliminary images of two members of the present sample (AGC 193953 and AGC 233638) have been obtained as part of this effort. In the interests of uniformity, we only derive quantitative results for the members of the present pilot sample from the SDSS images; the preliminary derivations of SDSS g-band magnitudes for AGC 193953 and AGC 233638 from the partially filled focal plane ODI (pODI) images agree within errors with the values derived from the original SDSS images.

2.3. Ultraviolet Observations

The ultraviolet (UV) properties of the five “Almost Dark” sources were derived using archival GALEX⁵ imaging. The depth of the GALEX images is heterogeneous across the sample; two sources (AGC 193953 and AGC 233638) have only All-Sky Imaging Survey depth imaging (~ 100 sec per integration), and one of these (AGC 193953) is a non-detection. The other three sources have deeper imaging (~ 1600 sec per integration); one source (AGC 208602) is a non-detection at this sensitivity level. Table 2 shows the magnitudes in the GALEX near and far ultraviolet channels, measured in identical apertures to those used to extract the optical photometry shown in Table 2. We use the far-UV fluxes to derive the recent (~ 100 Myr) star formation rates (SFR_{FUV}) of the sources using the prescriptions in Salim et al. (2007); these quantities are discussed in detail below.

3. The Gaseous and Stellar Components of the “Almost Dark” Sources

In this section we present the H I, optical, and UV images of each of the “Almost Dark” sources. We group these five systems into three categories: isolated systems (no known sources with coincident redshift within a projected distance of 400 kpc), systems with an apparent tidal origin, or systems near other objects.

³<http://www.noao.edu/wiyn/ODI/>

⁴<http://www.noao.edu/wiyn/>

⁵Based on observations made with the NASA Galaxy Evolution Explorer. GALEX is operated for NASA by the California Institute of Technology under NASA contract NAS5-98034.

3.1. Isolated Sources

We classify two of the five “Almost Dark” sources as isolated; no known sources with coincident redshift are located within a projected distance of 400 kpc of either source.

3.1.1. AGC 193953

AGC 193953 has the weakest ALFALFA H I line flux in this small sample ($S_{\text{HI}} = 0.43 \text{ Jy km s}^{-1}$; see Table 1). Located at $\sim 40 \text{ Mpc}$, the H I line width ($W_{50} = 32 \text{ km s}^{-1}$, where W_{50} is the width of the H I line at 50% of maximum) and H I reservoir of $1.6 \times 10^8 M_{\odot}$ are indicative of an average dwarf galaxy. This source was initially cataloged as a “dark” candidate due to the extremely low surface brightness nature of the optical counterpart, which is significantly displaced from the center of the ALFALFA beam. As discussed above, RFI compromised a number of channels in the datacube close to those that contain emission from the source. As such, the total H I flux in the VLA data ($0.13 \text{ Jy km s}^{-1}$) only amounts to $\sim 30\%$ of the ALFALFA flux; the H I properties (e.g., the more narrow range of velocities detected in the VLA data compared to the ALFALFA data) should only be considered to be representative based on these data.

Figure 2 shows the H I, SDSS-r band, and GALEX near-UV images of AGC 193953. At D configuration angular resolution the source is unresolved. The H I gas has a single surface density concentration that reaches a maximum column density of only $6.5 \times 10^{19} \text{ cm}^{-2}$. This surface density maximum is slightly offset spatially (though within one beam size) from the very low surface brightness optical counterpart, which is clearly visible in the SDSS-r band image. The Gaussian-fitted velocity field shows coherent and ordered rotation within the beam. As panels (b) and (d) of Figure 2 show, the isovelocity contours are parallel over $\sim 7 \text{ km s}^{-1}$ (~ 2 velocity resolution elements).

The optical counterpart of AGC 193953 is of very low surface brightness. As Tables 2 and 3 show, the SDSS integrated magnitudes imply a total B-band luminosity of $\sim 1.9 \times 10^7 L_{\odot}$ and a total stellar mass of $2.2 \times 10^6 M_{\odot}$. This faint stellar component is detected in the shallow GALEX near-UV image; while we have no direct constraints on the nature of recent star formation (which requires far-UV imaging), the faint nature of the source in the near-UV argues for quiescence over the most recent $\sim 100 \text{ Myr}$. Using the ALFALFA total H I flux and the SDSS-g and derived B-band luminosities, we derive $M_{\text{HI}}/L_g = 10$, $M_{\text{HI}}/L_B = 9$, and $M_{\text{HI}}/M_{\star} = 75$. While our analysis of the SDSS images have recovered more flux than the SDSS pipeline products, the source is close to the detection limits of the SDSS imaging; it is likely that deeper optical imaging would recover more low surface brightness

emission, thus decreasing the M_{HI}/L and M_{HI}/M_{\star} ratios.

3.1.2. AGC 208399

AGC 208399 is a very low surface brightness source that was included in the Huang et al. (2012) study of gas, stars, and star formation in ALFALFA dwarfs. AGC 208399 has the lowest recessional velocity of the five “Almost Dark” sources studied here; its flow model distance (see Table 1) is 10.1 Mpc. The flux integral ($S_{\text{HI}} = 1.06 \text{ Jy km s}^{-1}$) implies an H I mass of $2.6 \times 10^7 M_{\odot}$. By comparison with the properties in the Huang et al. (2012) sample, AGC 208399 is an extreme low surface brightness dwarf galaxy.

The H I, optical and UV images of AGC 208399 shown in Figure 3 reveal a centrally concentrated H I distribution that is spatially coincident with a diffuse, very low surface brightness optical counterpart in the SDSS r-band image. The VLA images recover $\sim 85\%$ of the ALFALFA flux integral. The H I column density peaks at $2.1 \times 10^{20} \text{ cm}^{-2}$ at $52''$ angular resolution, which marginally resolves the source. There is bulk rotation of the H I gas, extending across nearly 20 km s^{-1} . Most of this projected rotation is coherent, as evidenced by the nearly parallel isovelocity contours over most of the disk. However, there are some departures from circular motion in the outer regions, especially on the approaching side of the disk.

The GALEX imaging shown in Figure 3(c) shows a very low surface brightness blue component in close angular proximity to the H I surface density maximum. It is difficult to discern if this faint emission arises from the stellar population associated with AGC 208399 (and thus likely indicates recent star formation within the past $\sim 100 \text{ Myr}$) or with unrelated background sources; indeed, the SDSS-r image shown in panel (d) of Figure 3 reveals some small point sources that could be background star-forming galaxies. With this caution in mind, the UV fluxes are extracted using the same apertures as for the SDSS photometry (see Table 2). If the far-UV flux is associated with AGC 208399, then the implied $\text{SFR}_{\text{FUV}} = 5 \times 10^{-5} M_{\odot} \text{ yr}^{-1}$.

AGC 208399 shares many physical characteristics with the most massive dwarf galaxies in SHIELD (Cannon et al. 2011), a complementary ALFALFA follow-up observing campaign to study the physical properties of extremely low-mass systems cataloged by ALFALFA. Specifically, the SDSS colors, H I line widths, total H I masses, and distances of the most massive SHIELD galaxies are similar to those of AGC 208399. Interestingly, however, the majority of the SHIELD galaxies show evidence for recent star formation. The gas-rich ($M_{\text{HI}}/L_{\text{g}} = 6$; $M_{\text{HI}}/L_{\text{B}} = 5$; $M_{\text{HI}}/M_{\star} = 15$) but quiescent ($\text{SFR}_{\text{FUV}} = 5 \times 10^{-5} M_{\odot} \text{ yr}^{-1}$)

nature of AGC 208399 warrants further detailed exploration.

3.2. Systems With A Tidal Origin

3.2.1. AGC 208602

AGC 208602 was classified as a source with H I in the vicinity of, but offset from, an early-type galaxy (NGC 3457). A comparison of the ALFALFA detections near AGC 208602 with SDSS imaging revealed that this candidate “Almost Dark” source is located within 30’ of at least four known H I sources, including NGC 3443, NGC 3454, NGC 3455, and UGC 6022. This loose collection is part of the NGC 3370 group of galaxies, which is in turn part of the larger Leo II structure, which contains multiple gas-rich spirals and irregular galaxies. It also contains at least one early-type galaxy; NGC 3457 is in close angular proximity to AGC 208602, and its optical velocity ($V_{\text{sys}} = 1148 \text{ km s}^{-1}$; Cappellari et al. 2011) is in fair agreement with those of other members of the group (see below).

Figure 4 shows VLA H I and SDSS optical images of the region surrounding the “Almost Dark” candidate, AGC 208602. The size of the field of view ($\sim 36'$) is roughly equal to that of the primary beam of the VLA at H I. Within this field, five other H I line sources are detected in the velocity range immediately surrounding AGC 208602 (specifically, between $\sim 985 \text{ km s}^{-1}$ and $\sim 1210 \text{ km s}^{-1}$); these five sources are noted in each panel of Figure 4. In addition to NGC 3443, NGC 3454, NGC 3455, and UGC 6022, we also detect the neutral hydrogen in a small system labeled as SDSS J105506.66+172745.4. Each of these five sources shows coherent signatures of rotation.

Figure 5 shows a closer view of the detected H I from AGC 208602, and its relationship to NGC 3457. The neutral hydrogen in this source is of very low surface brightness, characterized by flocculent patches of emission that are at times disjoint in velocity space. While the VLA images recover $\sim 65\%$ of the ALFALFA flux, the integrated column densities at $49''$ resolution only reach the $\sim 5.5 \times 10^{19} \text{ cm}^{-2}$ level. The velocity structure of this source is sufficiently incoherent that attempts to fit Gaussians to the emission in the cube failed. Thus, the moment one maps shown in Figures 4 and 5 were derived by standard routines. Emission is detected over $\sim 50 \text{ km s}^{-1}$; there is no convincing evidence of coherent rotation of this source in the velocity field or in the 3-dimensional cube.

The SDSS and GALEX images of AGC 208602 presented in Figure 5 reveal no detectable optical counterpart. The magnitudes derived in Table 2 are thus listed as limits; the corresponding luminosities, M_{HI}/L ratios ($M_{\text{HI}}/L_{\text{g}} > 48$; $M_{\text{HI}}/L_{\text{B}} > 45$), and M_{HI}/M_{\star} ratio (> 49) should likewise be considered limiting values. Deeper optical imaging of this source might

be fruitful, but the interpretation may be complicated by the outer halo of NGC 3457.

AGC 208602 stands out markedly in Table 3; it has the largest M_{HI}/L ratios of any of the five sources in the present work. Further, the irregular morphology and incoherent velocity structure are unlike those found in any of the other systems studied here or in other low-mass galaxies. Based on these factors, and on the source’s membership in the NGC 3370 Group, we conclude that this feature may have a tidal origin. It shares some physical characteristics with other ALFALFA-detected groups with extended tidal structures (e.g., Lee-Waddell et al. 2014 and references therein).

It is not clear which sources in the NGC 3370 Group might have interacted to give rise to this object. At the adopted distance of 18.5 Mpc, the $1.2 \times 10^8 M_{\odot}$ of H I associated with AGC 208602 spans more than 20 kpc. This remarkable cloud is located roughly 65 kpc from UGC 6022 and SDSS J105506.66+172745.4, the two gas-rich systems with the closest angular projection on the sky. Further, AGC 208602 is located between NGC 3443 (~ 126 kpc projected separation) and the early-type galaxy NGC 3457 (~ 15 kpc projected separation); it may be the case that the feature was associated with NGC 3443, and that a recent close encounter with NGC 3457 has stripped the H I away from NGC 3443. A very deep single-dish map of the entire NGC 3370 Group might be fruitful; this would provide sensitivity to possible low surface brightness tidal structure.

3.3. Systems Near Other Galaxies

The remaining two “Almost Dark” sources are located in sufficiently close angular proximity to other known sources that the assignment of an unambiguous optical counterpart was not possible using the ALFALFA data alone.

3.3.1. AGC 226178

AGC 226178 is an H I source with no optical counterpart at the ALFALFA centroid. The system is a possible member of the Virgo Cluster; Kent et al. (2008) catalog its H I properties, but find no optical counterpart. They note the possible association with AGC 229166, an optically faint, low surface brightness object (not detected in H I by ALFALFA, but cataloged as an AGC galaxy based on the extended optical emission which was apparent when examining the ALFALFA data) located at $(\alpha, \delta) = (12^h 46^m 41.7^s, 10^\circ 23' 09'')$, roughly $2.3'$ from the ALFALFA centroid for AGC 226178. The VLA images presented here show the H I centroid to be $1'$ south of AGC 229166, and suggest that the H I is associated with

a second possible optical/UV counterpart with an irregular morphology.

AGC 226178 is in close angular and velocity proximity to other H I-bearing sources in our spectral line data. As shown in Figure 6, two other Virgo dwarf galaxies are detected at high significance: VCC 2034 (AGC 221001; $V_{\text{sys}} = 1504 \text{ km s}^{-1}$; angular separation $\simeq 910''$ $\simeq 72.8 \text{ kpc}$) and VCC 2037 (AGC 221004; $V_{\text{sys}} = 1142 \text{ km s}^{-1}$; angular separation $\simeq 720''$ $\simeq 57.5 \text{ kpc}$). We do not find clear evidence for an ongoing interaction between any of these sources at our current sensitivity level.

At SDSS imaging depths, the optical counterpart of the AGC 226178 H I source is ambiguous. To highlight the low surface brightness nature of both AGC 226178 and AGC 229166, panel (d) of Figure 6 shows the SDSS-r band image from panel (b), smoothed by a Gaussian kernel with $\sigma = 3$ pixels. The H I is coincident with a very faint irregular optical counterpart candidate, but offset from AGC 229166. Figure 7 shows the H I, optical, and UV properties in a smaller region containing only these two sources; note that the SDSS-r band image in this figure is the same as shown in panel (d) of Figure 6 (i.e., it has been smoothed by a Gaussian kernel). The optical morphology of the possible stellar counterpart is highly irregular, appearing as a number of low surface brightness knots of emission oriented from southwest to northeast. Remarkably, this same morphology is apparent in the color GALEX image presented in panel (c); the blue color is indicative of a significant far-UV flux. Note that AGC 229166 is not detected with significance in the GALEX images.

The H I associated with AGC 226178 shows properties that are akin to those of low-mass dwarf galaxies. The neutral hydrogen is centrally concentrated, reaching a maximum column density of $1 \times 10^{20} \text{ cm}^{-2}$. While the source is unresolved by these VLA observations, there is a clearly defined velocity gradient spanning $\sim 10 \text{ km s}^{-1}$. The total ALFALFA flux integral implies an H I mass of $\sim 4 \times 10^7 M_{\odot}$. Our VLA images recover $\sim 40\%$ of this flux; there is minor contamination from RFI, but it is likely that some of the H I detected by Arecibo is distributed over larger angular scales than those probed by the present VLA observations.

The optical and UV properties of AGC 226178 are extracted at the position of the H I centroid and using the parameters given in Table 2. Note that the elliptical aperture size closely matches the UV and optical morphology of the source. Using the SDSS images, we derive $M_{\text{HI}}/L_g = 7$; $M_{\text{HI}}/L_B = 6$, and $M_{\text{HI}}/M_{\star} = 30$. The far-UV flux implies a recent $\text{SFR}_{\text{FUV}} = 0.0017 M_{\odot} \text{ yr}^{-1}$.

We conclude that the H I source AGC 226178 is a dwarf galaxy. We base this conclusion on two primary lines of evidence. First, there is excellent positional agreement between the H I centroid and the UV-bright stellar component. Second, the UV morphology of the putative stellar component suggests an inclined disk morphology. Assuming circular

rotation, the orientation of this disk is perpendicular to the isovelocity contours shown in Figure 7(d); this is exactly what would be expected in a rotating disk seen nearly edge-on.

If the H I source AGC 226178 were instead associated with the very low surface brightness object labeled as AGC 229166 in Figures 6 and 7, then significant interpretive challenges would arise. First, the excellent positional and kinematic agreements noted above would need to occur by chance with an unrelated background source. Second, the $\sim 1'$ angular offset between the H I source and the centroid of AGC 229166 corresponds to a minimum ~ 5 kpc physical separation (assuming AGC 226178 and AGC 229166 are at the same distance); moving $\sim 10^7 M_\odot$ of H I over such a distance would require energies that could likely only arise during a gravitational interaction or ram pressure stripping event.

An alternative but speculative interpretation is one in which AGC 226178 and AGC 229166 are in fact the same physical system. There are very weak suggestions of spiral structure in the smoothed SDSS-r band image of AGC 229166 shown in Figure 7(d). It is conceivable that this is a nearly face-on, gas-poor system. In such a scenario, AGC 226178 could be an outer spiral arm that has experienced some sort of infall or interaction episode that has ignited recent star formation. While such a scenario seems physically unlikely, it cannot be completely ruled out with the present data.

3.3.2. AGC 233638

AGC 233638 was classified as a pair of galaxies with very low optical surface brightness. It is the most distant source in our pilot sample. The total ALFALFA H I flux integral (of which $\sim 65\%$ is recovered in our VLA observations) implies an H I mass of $3.3 \times 10^9 M_\odot$. Figure 8 shows that the VLA observations resolve these two sources (AGC 233638 and AGC 743043), which are separated by $\sim 3.3'$ (~ 108 kpc at the adopted distance of 112 Mpc) and by less than 100 km s^{-1} . The SDSS-r band imaging allows a clear identification of an associated optical counterpart with each H I peak. AGC 233638 was included in the “Almost Dark” sample due to the ambiguous nature of multiple possible optical counterparts; the higher spatial resolutions presented here allow us to characterize the source with confidence.

As Figure 9 shows, the candidate “Almost Dark” source is a star-forming dwarf irregular galaxy. There is coherent and well-ordered rotation spanning a projected velocity width of $\sim 40 \text{ km s}^{-1}$. The H I surface density maximum is exactly co-spatial with the GALEX centroid. While the GALEX images are shallow, they nonetheless allow a robust measurement of the UV fluxes in both bands (see SDSS and GALEX photometry in Table 2). Based on the far-UV flux, this source has undergone significant star formation during the most recent

~ 100 Myr ($\text{SFR}_{\text{FUV}} = 0.05 \text{ M}_{\odot} \text{ yr}^{-1}$). The $\text{M}_{\text{HI}}/\text{L}$ and $\text{M}_{\text{HI}}/\text{M}_{\star}$ ratios for AGC 233638 are typical of those found in star-forming galaxies: $\text{M}_{\text{HI}}/\text{L}_{\text{g}} = 3$, $\text{M}_{\text{HI}}/\text{L}_{\text{B}} = 3$, $\text{M}_{\text{HI}}/\text{M}_{\star} = 14$. We conclude that AGC 233638 is a very intriguing star-forming dwarf irregular galaxy; it has an absolute magnitude ($\text{M}_{\text{B}} \simeq -17$) roughly equal to that of the Large Magellanic Cloud, a total H I mass ($\text{M}_{\text{HI}} = 3.2 \times 10^9 \text{ M}_{\odot}$) roughly equal to that of the Milky Way, and a stellar mass ($\text{M}_{\star} = 2.2 \times 10^8 \text{ M}_{\odot}$) typical of those found in dwarf galaxies.

A bright nuclear point source is coincident with the optical counterpart of AGC 233638; an SDSS spectrum of this bright central knot is available. The SDSS pipeline software proposes a redshift of $z=0.940$. Inspection of the SDSS spectrum suggests that this high-redshift classification may be erroneous; no obvious emission or absorption lines agree with this redshift. Further, this would be highly inconsistent with the present observations of the velocity of the neutral interstellar medium. If this compact source is not associated with AGC 233638 itself, then the optical luminosity and resulting stellar mass of AGC 233638 will both decrease, raising the $\text{M}_{\text{HI}}/\text{L}$ and $\text{M}_{\text{HI}}/\text{M}_{\star}$ ratios. Follow-up optical spectroscopy of this compact source would be very valuable.

4. Discussion

4.1. The “Almost Dark” Sources in Context

The five “Almost Dark” sources studied in this work are representative of the sample of ALFALFA-discovered systems that are not uniquely identified with optical counterparts using ALFALFA data alone. As a result, most harbor unusually high H I mass to light ratios. In the present work, we use multi-wavelength follow-up observations to determine the nature of these objects: 4 sources are likely galaxies, while one source is likely a tidal remnant.

Keeping in mind the uncertainties that arise because different works have measured optical properties in different ways, the systems studied here can be compared to both the sample of ALFALFA dwarf galaxies in Huang et al. (2012) and to the full $\alpha.40$ database presented in Haynes et al. (2011). In Figure 10 we thus show the logarithm of the $\text{M}_{\text{HI}}/\text{M}_{\star}$ ratio versus the logarithm of the stellar mass for all of these systems. There is a clear trend for higher $\text{M}_{\text{HI}}/\text{M}_{\star}$ ratios in systems of fainter absolute magnitude (lower stellar mass), although the scatter is significant (becoming more pronounced as stellar mass decreases). With the exception of AGC 208399, the five sources studied here preferentially populate the extreme upper left region of this plot; these are gas-rich systems with low stellar masses.

A second comparison can be made against targeted studies of gas-rich, low surface

brightness dwarf galaxies. For example, van Zee et al. (1997) computes the M_{HI}/L ratios in a sample of seven low surface brightness dwarfs and a comparison sample of five dwarfs with more typical hydrogen mass to light ratios. All twelve of these systems have M_{HI}/L_B values near unity (the lowest ratio being 0.6 in UGC 891 and the highest ratio being 6.0 in UGC 5716). The M_{HI}/L_B values of the four “Almost Dark” systems in the present study that appear to be bona fide galaxies (see Table 3) range from 3 (AGC 233638) to 9 (AGC 193953). The galaxies in the present work thus harbor M_{HI}/L_B that are comparable to the most extreme systems in van Zee et al. (1997).

Further comparisons can be made with studies of low surface brightness galaxies that display elevated M_{HI}/L ratios (e.g., Longmore et al. 1982; van Zee et al. 1995; de Blok et al. 1996; Matthews & Gallagher 1997; O’Neil et al. 2000; Doyle et al. 2005). While some physical characteristics of the present “Almost Dark” objects are similar to those found for objects in these previous studies, the ALFALFA “Almost Dark” sources constitute a different class of object. For example, all of the low surface brightness sources in the de Blok et al. (1996) sample that are within the ALFALFA footprint are detected in H I, and all of them are assigned an optical counterpart by comparison with SDSS imaging. In contrast, the ALFALFA “Almost Dark” sources represent the most extreme objects ($<0.5\%$ of the full ALFALFA catalog) for which an optical counterpart remains elusive, even when comparing the sensitive ALFALFA and SDSS/DSS2B survey products.

4.2. The Physical Characteristics of the “Almost Dark” Sources

It is tempting to study the nature of the recent (within ~ 100 Myr) star formation in those systems in which star formation is apparent based on a measurable GALEX far-UV flux (AGC 208399, AGC 226178, AGC 233638). However, with the angular resolution afforded by these D configuration observations, all of these sources are only marginally resolved (if at all). The resulting H I column densities and corresponding mass surface densities will necessarily be lower limits that will increase upon observation at higher angular resolution. Taken at face value, the observed column density maxima [$N_{\text{HI}} = (1-2) \times 10^{20} \text{ cm}^{-2}$; see Figures 3, 7, and 9] are significantly lower than the peak column densities observed in the more nearby galaxies of the van Zee et al. (1997) sample [$N_{\text{HI}} = (7-30) \times 10^{20} \text{ cm}^{-2}$]. Higher spatial resolution observations of these “Almost Dark” sources would be valuable for studying the nature of the star formation law in the extreme M_{HI}/L regime by allowing us to resolve the H I surface densities in the disks and correlating these values with well-understood tracers of ongoing star formation.

The elevated M_{HI}/L and M_{HI}/M_\star ratios in the four non-tidal “Almost Dark” candidates

raise interesting questions about galaxy evolution. The H I masses are not unusually low for any of these sources; as with all known non-spheroidal galaxies, an H I reservoir larger than $10^7 M_{\odot}$ appears to be at least partially converted into stars. However, in these sources, this conversion appears to be extremely inefficient. Using the UV-based SFRs tabulated in Table 3, the gas consumption timescales exceed the Hubble time for all sources. These “Almost Dark” galaxies are an extreme case of inefficient star formation, similar to, but more dramatic than, what is found in the outer regions of spiral disks and in gas-dominated dwarfs (c.f., Bigiel et al. 2008).

The angular resolution of the H I observations presented here results in physical resolution elements ranging from 2.5 kpc (AGC 208399) to 32.6 kpc (AGC 233638). This precludes rotation curve work and a detailed mass decomposition. It is interesting to note in this context that the objects identified as galaxies do show irregular kinematics and morphology compared to dynamically relaxed systems. For example, AGC 208399 and AGC 226178 show lopsided kinematics; AGC 193953 shows a misalignment between the total H I intensity and the kinematical axes; AGC 223638 may be warped or show symmetric (bar-like) streaming motions. Higher resolution observations of the nearest of these sources would facilitate an examination of the dark and baryonic components in these systems.

5. Conclusions and Outlook

We have presented new H I spectral line observations of five sources extracted from the ALFALFA catalog as being representative members of the “Almost Dark” population: systems for which an optical counterpart cannot be assigned using ALFALFA data alone. These sources harbor extreme hydrogen mass to optical luminosity ratios. With the optical, UV, and interferometric H I imaging presented in this work, we now have a much more clear understanding of the nature of these objects; none of them appears to be a bona fide “dark galaxy”.

The H I images of these sources localize the H I gas and provide a coarse representation of the rotation and dynamics of the neutral interstellar medium. We compare these H I results with SDSS and GALEX imaging. In four of the five systems, a stellar counterpart is detected that is co-spatial with the H I centroid. Each of these objects shows signatures of coherent rotation; we classify these systems as galaxies.

One system in this study (AGC 208602) lacks a detectable stellar population in SDSS and GALEX imaging. This source has the largest M_{HI}/L ratio in our sample, has an irregular H I morphology, and lacks clear signs of coherent rotation. Given its location in the NGC 3370

group, we conclude that this feature has a tidal origin.

The gaseous and stellar components of AGC 226178 make it a very intriguing system. It is located within a projected separation of ~ 75 kpc from VCC 2034 and VCC 2037, both of which are detected in our H I imaging. It is also in very close angular projection ($\sim 1'$, or ~ 5 kpc at the adopted distance) to AGC 229166, a source with very low optical surface brightness that is not detected in H I by either ALFALFA or the present observations or in the UV in GALEX imaging. Surprisingly, these GALEX images reveal a significant UV flux from an irregular-morphology source that is coincident with the H I centroid of AGC 226178. We interpret this source as the stellar counterpart of AGC 226178 and thus classify it as a dwarf galaxy. The nature of AGC 229166, and its possible association with AGC 226178, remains unclear with the present data.

The remaining three sources in this study (AGC 193953, AGC 208399, and AGC 233638) appear to be galaxies with higher than average M_{HI}/L ratios in comparison with those found in the samples of van Zee et al. (1997), Haynes et al. (2011), and Huang et al. (2012). Of these sources, AGC 193953 and AGC 208399 are the most promising for more detailed investigation. With the highest M_{HI}/L ratios of the galaxies in this study, and very low UV-based star formation rates, these sources can facilitate an exploration of the star formation threshold in a sparsely-explored region of parameter space. AGC 233638 is a comparatively distant source with a lower mass to light ratio; higher resolution observations of this source will be less valuable.

As of this writing, there are roughly 50 viable “Almost Dark” candidate sources in the ALFALFA catalog. The present pilot study of five sources from this larger sample demonstrates the complexity of the members of this heterogeneous class of objects: the higher angular resolution VLA images localize the H I gas (thereby facilitating an association with a stellar component for most of these objects) and reveal ordered motions indicative of galaxy-like objects. The discovery potential of a dedicated follow-up observing campaign to study the gaseous components of all candidate “Almost Dark” systems is thus exceptionally high.

Our team is pursuing similar H I observations of the full “Almost Dark” sample, as well as deep optical images of the sources with large field-of-view instruments. For example, preliminary results from these initiatives demonstrate significant similarities between AGC 226178 (studied here) and AGC 229385 and its neighbors (Janowiecki et al., in preparation). These future works hold significant promise for furthering our understanding of the evolution of extremely gas-rich systems. They will allow us to explore the nature of star formation in the high M_{HI}/L regime; the preliminary results from the present work suggest a very inefficient or suppressed star formation process. Most importantly, these endeavors will allow us to quantify the frequency of truly “dark” galaxies (if they exist), using the

statistically robust ALFALFA database with well-understood sensitivity and completeness limits.

J.M.C. is supported by NSF grant 1211683. J.M.C., R.A.K., C.P.M., N.N., and P.T. acknowledge NSF grant AST-1211005. The ALFALFA work at Cornell is supported by NSF grant AST-1107390 and by the Brinson Foundation. K.L.R. acknowledges support from NSF grant AST-0847109. J.M.C. would like to thank the Instituto Nazionale di Astrofisica and the Osservatorio Astronomico di Padova for their hospitality during a productive sabbatical leave. L.L. would like to thank Angus Wright for technical support using his code, LAMB-DAR. G.J. started to participate in this project as an employee of ASTRON, Dwingeloo, The Netherlands (Nederlandse Organisatie voor Wetenschappelijk Onderzoek, NWO). This investigation has made use of the NASA/IPAC Extragalactic Database (NED) which is operated by the Jet Propulsion Laboratory, California Institute of Technology, under contract with the National Aeronautics and Space Administration, and NASA's Astrophysics Data System. This investigation has made use of data from the Sloan Digital Sky Survey (SDSS). Funding for the SDSS and SDSS-II has been provided by the Alfred P. Sloan Foundation, the Participating Institutions, the National Science Foundation, the U.S. Department of Energy, the National Aeronautics and Space Administration, the Japanese Monbukagakusho, the Max Planck Society, and the Higher Education Funding Council for England. The SDSS Web Site is <http://www.sdss.org/>.

The SDSS is managed by the Astrophysical Research Consortium for the Participating Institutions. The Participating Institutions are the American Museum of Natural History, Astrophysical Institute Potsdam, University of Basel, University of Cambridge, Case Western Reserve University, University of Chicago, Drexel University, Fermilab, the Institute for Advanced Study, the Japan Participation Group, Johns Hopkins University, the Joint Institute for Nuclear Astrophysics, the Kavli Institute for Particle Astrophysics and Cosmology, the Korean Scientist Group, the Chinese Academy of Sciences (LAMOST), Los Alamos National Laboratory, the Max-Planck-Institute for Astronomy (MPIA), the Max-Planck-Institute for Astrophysics (MPA), New Mexico State University, Ohio State University, University of Pittsburgh, University of Portsmouth, Princeton University, the United States Naval Observatory, and the University of Washington.

REFERENCES

- Adams, E.A.K., Faerman, Y., Oosterloo, T. A., et al. 2014, A&A, submitted
- Ahn, C. P., Alexandroff, R., Allende Prieto, C., et al. 2014, ApJS, 211, 17
- Bigiel, F., Leroy, A., Walter, F., et al. 2008, AJ, 136, 2846
- Blanton, M. R., & Roweis, S. 2007, AJ, 133, 734
- Cannon, J. M., Giovanelli, R., Haynes, M. P., et al. 2011, ApJ, 739, L22
- Cappellari, M., Emsellem, E., Krajnović, D., et al. 2011, MNRAS, 413, 813
- de Blok, W. J. G., McGaugh, S. S., & van der Hulst, J. M. 1996, MNRAS, 283, 18
- Dowell, J. D. 2010, Ph.D. Thesis, Indiana University
- Doyle, M. T., Drinkwater, M. J., Rohde, D. J., et al. 2005, MNRAS, 361, 34
- Duc, P.-A., & Bournaud, F. 2008, ApJ, 673, 787
- English, J., Koribalski, B., Bland-Hawthorn, J., Freeman, K. C., & McCain, C. F. 2010, AJ, 139, 102
- Giovanelli, R., Haynes, M. P., Kent, B. R., et al. 2005, AJ, 130, 2598
- Haynes, M. P., Giovanelli, R., & Kent, B. R. 2007, ApJ, 665, L19
- Haynes, M. P., Giovanelli, R., Martin, A. M., et al. 2011, AJ, 142, 170
- Huang, S., Haynes, M. P., Giovanelli, R., et al. 2012, AJ, 143, 133
- Jorsater, S., & van Moorsel, G. A. 1995, AJ, 110, 2037
- Kent, B. R., Giovanelli, R., Haynes, M. P., et al. 2008, AJ, 136, 713
- Kent, B. R., Spekkens, K., Giovanelli, R., et al. 2009, ApJ, 691, 1595
- Kent, B. R. 2010, ApJ, 725, 2333
- Lee-Waddell, K., Spekkens, K., Cuillandre, J.-C., et al. 2014, MNRAS, 443, 3601
- Longmore, A. J., Hawarden, T. G., Goss, W. M., Mebold, U., & Webster, B. L. 1982, MNRAS, 200, 325
- Martin, D. C., Fanson, J., Schiminovich, D., et al. 2005, ApJ, 619, L1

- Martin, A. M., Papastergis, E., Giovanelli, R., et al. 2010, *ApJ*, 723, 1359
- Martin, A. M., Giovanelli, R., Haynes, M. P., & Guzzo, L. 2012, *ApJ*, 750, 38
- Masters, K. L. 2005, Ph.D. Thesis, Cornell University
- Matsuoka, Y., Ienaka, N., Oyabu, S., Wada, K., & Takino, S. 2012, *AJ*, 144, 159
- Matthews, L. D., & Gallagher, J. S., III 1997, *AJ*, 114, 1899
- Mihos, J. C., Keating, K. M., Holley-Bockelmann, K., Pisano, D. J., & Kassim, N. E. 2012, *ApJ*, 761, 186
- Minchin, R., Davies, J., Disney, M., et al. 2005, *ApJ*, 622, L21
- Minchin, R., Davies, J., Disney, M., et al. 2007, *ApJ*, 670, 1056
- O’Neil, K., Bothun, G. D., & Schombert, J. 2000, *AJ*, 119, 136
- Oosterloo, T. A., Heald, G. H., & de Blok, W. J. G. 2013, *A&A*, 555, L7
- Papastergis, E., Martin, A. M., Giovanelli, R., & Haynes, M. P. 2011, *ApJ*, 739, 38
- Salim, S., Rich, R. M., Charlot, S., et al. 2007, *ApJS*, 173, 267
- Schlaafly, E. F., & Finkbeiner, D. P. 2011, *ApJ*, 737, 103
- Serra, P., Koribalski, B., Duc, P.-A., et al. 2013, *MNRAS*, 428, 370
- van Zee, L., Haynes, M. P., & Giovanelli, R. 1995, *AJ*, 109, 990
- van Zee, L., Haynes, M. P., Salzer, J. J., & Broeils, A. H. 1997, *AJ*, 113, 1618
- Walter, F., Skillman, E. D., & Brinks, E. 2005, *ApJ*, 627, L105
- Walter, F., Brinks, E., de Blok, W. J. G., et al. 2008, *AJ*, 136, 2563
- Zibetti, S., Charlot, S., & Rix, H.-W. 2009, *MNRAS*, 400, 1181

Table 1. Basic and Global HI Properties of the Candidate “Almost Dark” Systems

AGC Number	RA ^a (J2000)	Dec ^a (J2000)	Offset ^b (arcmin)	S _{HI} ^c (Jy km s ⁻¹)	V _{sys} (km s ⁻¹)	W ₅₀ (km s ⁻¹)	D ^d (Mpc)	log(M _{HI}) (M _⊙)
193953 ^e	143.6444	12.394	1.32	0.43	2591	32	39.9	8.21
208399 ^e	160.0417	4.910	0.36	1.06	747	31	10.1	7.41
208602 ^f	163.6558	17.635	0.92	1.45	1093	50	18.5	8.07
226178 ^{e,g}	191.6782	10.369	1.33	0.62	1581	28	16.5	7.60
233638 ^e	202.8267	16.167	0.05	1.10	7587	62	112	9.51

^aRA and Dec of the H I centroid measured in the VLA images.

^bAngular offsets between ALFALFA centroid coordinates and VLA centroid coordinates.

^cTotal integrated H I line flux density measured by ALFALFA in Jy km s⁻¹.

^dDistances based on the local flow model by Masters (2005) and Martin et al. (2010).

^eVery low surface brightness optical counterpart.

^fPositional offset from early-type galaxy NGC 3457.

^gMultiple possible optical counterparts.

Table 2. Observed Properties of the Candidate “Almost Dark” Systems

AGC Number	Aperture ^a Size	m _{FUV} ^b (mag.)	m _{NUV} ^c (mag.)	m _{g,SDSS} ^d (mag.)	m _g ^e (mag.)	m _r ^f (mag.)
193953	16″×11″	N/A	20.0±0.3	20.8±0.1	20.2±0.3	20.1±0.3
208399	26″×18″	21.6±0.3	19.9±0.3	20.00±0.03	18.6±0.2	18.3±0.2
208602	15″×15″	>21.4	20.3±0.3	—	>20.5	>21.0
226178	42″×8″	19.6±0.2	20.2±0.3	22.4±0.1	19.4±0.3	19.2±0.3
233638	25″×18″	19.9±0.2	19.3±0.2	18.72±0.01	18.0±0.2	17.8±0.2

^aSemi-major and semi-minor axis lengths of photometric aperture.

^bApparent integrated magnitude of the source in the GALEX FUV band. No Galactic absorption correction has been applied.

^cApparent integrated magnitude of the source in the GALEX NUV band. No Galactic absorption correction has been applied.

^dSDSS catalog model magnitude.

^eApparent integrated magnitude of the source in the SDSS g band. No Galactic absorption correction has been applied.

^fApparent integrated magnitude of the source in the SDSS r band. No Galactic absorption correction has been applied.

Table 3. Derived Properties of the Candidate “Almost Dark” Systems

AGC Number	L_g^a (L_\odot)	L_B^b (L_\odot)	M_\star^c (M_\odot)	M_{HI}/L_g^d (M_\odot/L_\odot)	M_{HI}/L_B^e (M_\odot/L_\odot)	M_{HI}/M_\star^f (M_\odot/M_\odot)	SFR_{FUV}^g ($M_\odot \text{ yr}^{-1}$)
193953	1.6×10^7	1.9×10^7	2.2×10^6	10	9	75	...
208399	4.4×10^6	5.0×10^6	1.7×10^6	6	5	15	5.1×10^{-5}
208602	$<2.6 \times 10^6$	$<2.8 \times 10^6$	$<2.5 \times 10^6$	>48	>45	>49	$<2.6 \times 10^{-4}$
226178	5.7×10^6	6.7×10^6	1.3×10^6	7	6	30	0.0017
233638	9.6×10^8	1.1×10^9	2.2×10^8	3	3	14	0.047

^ag-band luminosity, corrected for Galactic extinction via Schlafly & Finkbeiner (2011), derived from g band magnitudes extracted from downloaded SDSS images using LAMBDAR.

^bB-band luminosity, corrected for Galactic extinction via Schlafly & Finkbeiner (2011), derived from g and r band magnitudes extracted from downloaded SDSS images using LAMBDAR.

^cStellar mass, derived using the LAMBDAR r-band magnitudes, g-r colors, and the formalism in Zibetti et al. (2009).

^dRatio of H I mass in M_\odot to SDSS g-band luminosity in L_\odot .

^eRatio of H I mass in M_\odot to B-band luminosity in L_\odot .

^fRatio of H I mass in M_\odot to stellar mass in M_\odot .

^gFar-UV star formation rate.

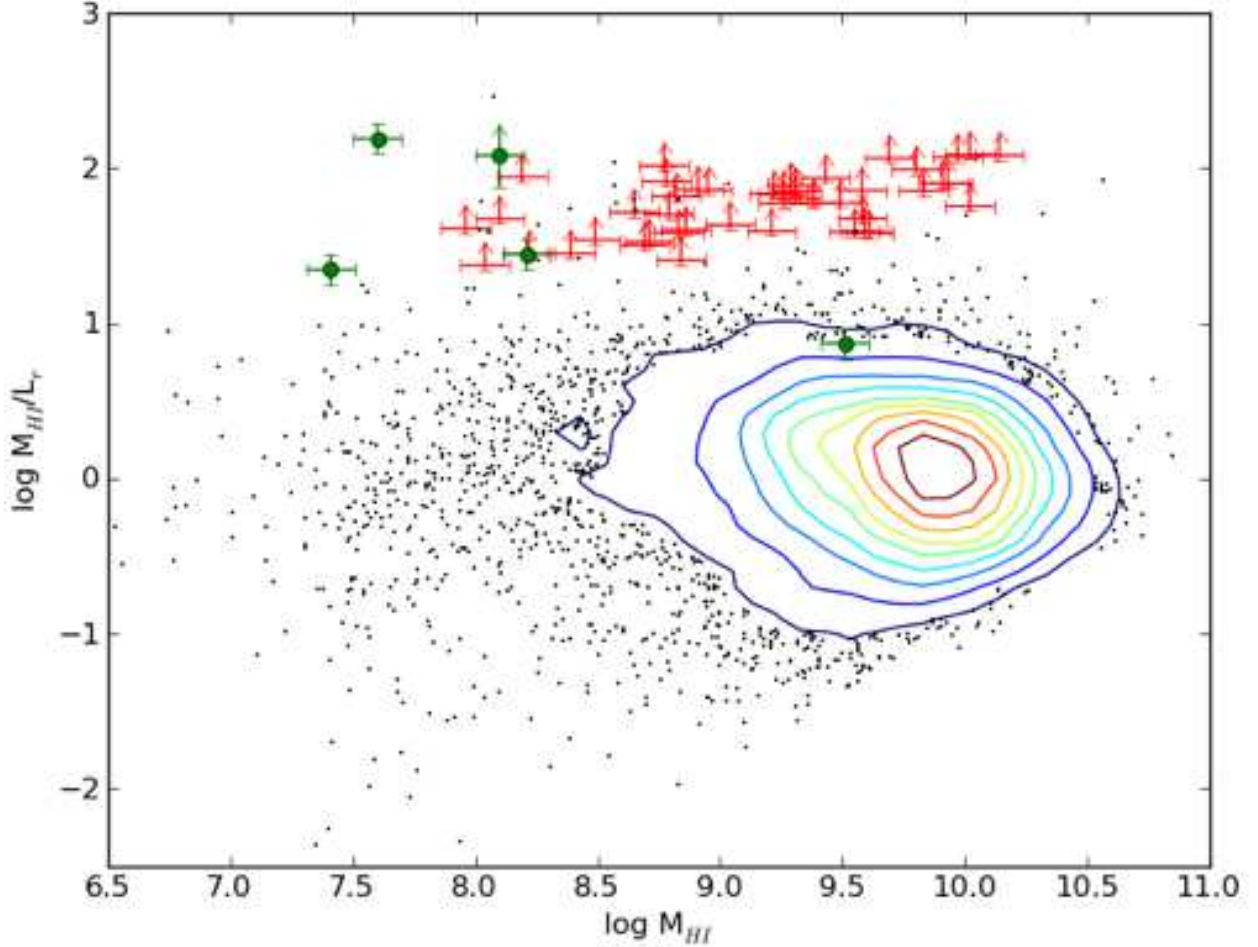


Fig. 1.— Plot of the logarithm of the neutral hydrogen to optical luminosity ratio, $M_{\text{HI}}/L_{\text{B}}$, versus the logarithm of the H I mass, for all members of the $\alpha.40$ catalog (Haynes et al. 2011). All black points and areas within contours represent galaxies with reliable SDSS optical counterparts. The contours show number densities in intervals of 10%, from 10% to 90% of the number density maximum (which occurs at $\log(M_{\text{HI}}) = 9.8$; see Haynes et al. 2011). The candidate “Almost Dark” sources are shown in red or green (studied in this work). These sources have high M_{H}/L but lack obvious or uncertain optical counterparts. The green point at $\log(M_{\text{HI}}) = 9.51$ is AGC 233638, a massive H I source with a discrepant SDSS redshift whose association was uncertain based on ALFALFA alone; see detailed discussion in § 3.3.2. For consistency, all M_{HI}/L values calculated here use SDSS catalog magnitudes.

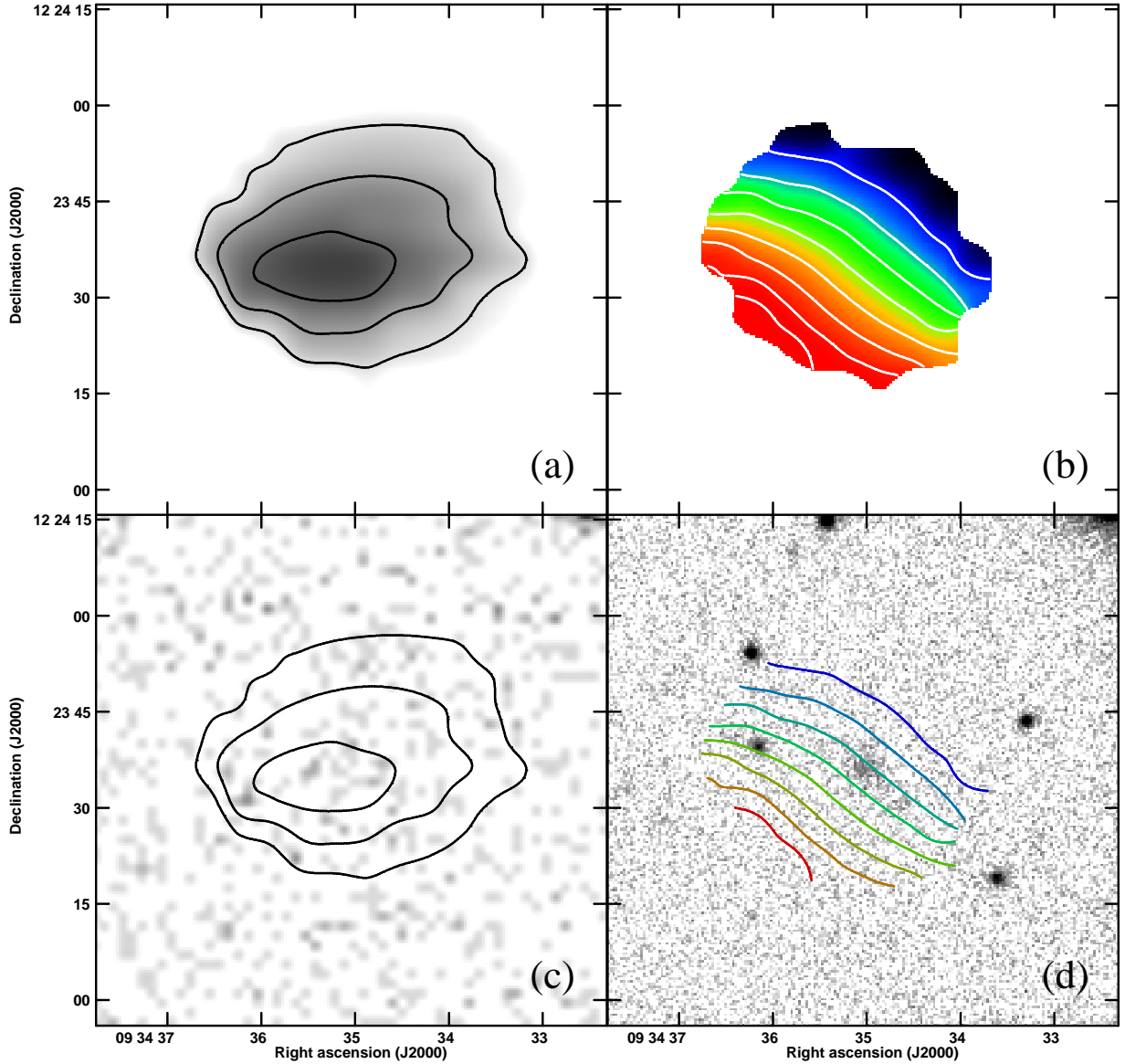


Fig. 2.— H I, SDSS R-band, and GALEX images of AGC 193953. Panel (a) shows H I column density contours at the $(0.4, 0.5, 0.6) \times 10^{20} \text{ cm}^{-2}$ levels, overlaid on a greyscale representation of the image. Panel (b) shows H I isovelocity contours from 2596 km s^{-1} to 2603 km s^{-1} in intervals of 1 km s^{-1} , overlaid on a color representation of the velocity field image. Panel (c) shows the GALEX near-UV image, while panel (d) shows the SDSS r-band image (displayed in a logarithmic stretch to highlight low surface brightness emission); the contours in (c) are the same as in panel (a), while the contours in (d) are the same as in panel (b). The velocity field was derived by fitting Gaussian functions to the full data cube. The H I beam size is $50''$; the source is unresolved at this angular resolution.

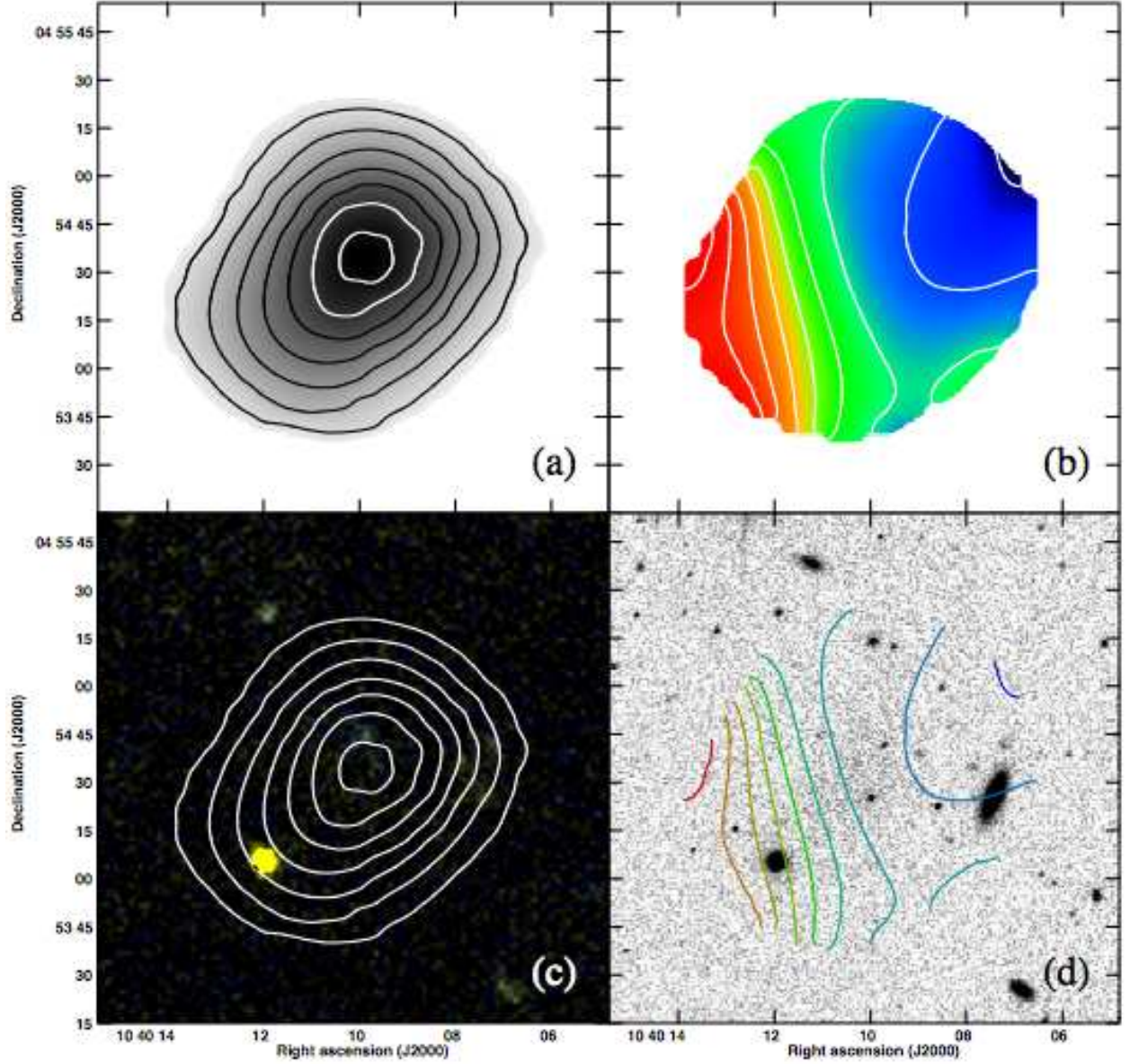


Fig. 3.— H I, SDSS R-band, and GALEX images of AGC 208399. Panel (a) shows H I column density contours at the $(0.5, 0.75, 1.0, 1.25, 1.5, 1.75, 2.0) \times 10^{20} \text{ cm}^{-2}$ levels, overlaid on a greyscale representation of the image. Panel (b) shows H I isovelocity contours from 760 km s^{-1} to 776 km s^{-1} in intervals of 2 km s^{-1} , overlaid on a color representation of the velocity field image. Panel (c) shows a color representation of the GALEX UV images, while panel (d) shows the SDSS r-band image (displayed in a logarithmic stretch to highlight low surface brightness emission); the contours in (c) are the same as in panel (a), while the contours in (d) are the same as in panel (b). The velocity field was derived by fitting Gaussian functions to the full data cube. The H I beam size is $52''$; the source is marginally resolved at this angular resolution. The two galaxies in panel (d) located close to AGC 208399 (to the W and SW) are background galaxies with SDSS redshifts of 0.065 and 0.071, respectively.

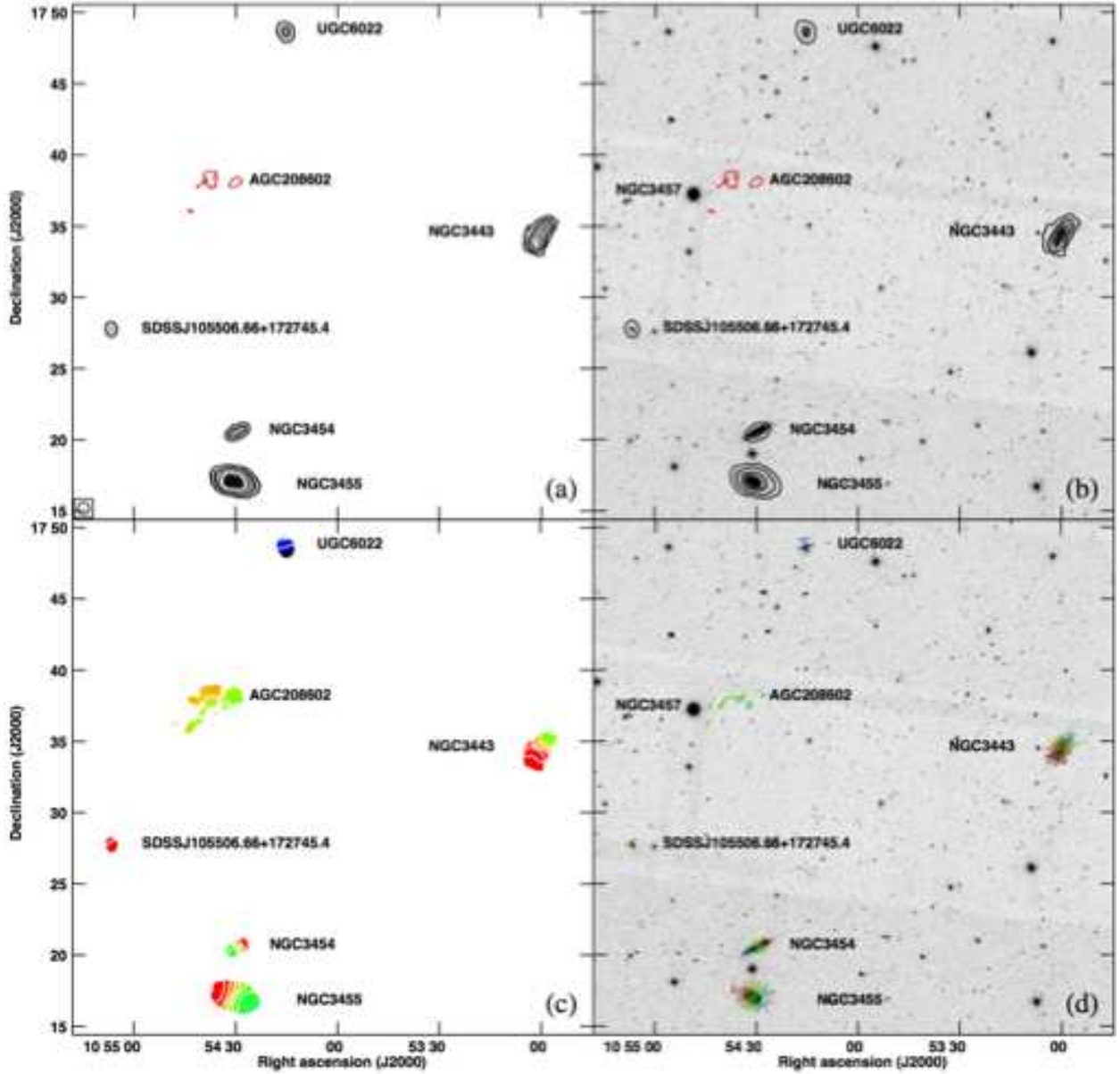


Fig. 4.— H I and SDSS R-band images of the AGC 208602 field. Panel (a) shows H I column density contours overlaid at the $3.5 \times 10^{19} \text{ cm}^{-2}$ level (red, highlighting the low surface brightness nature of AGC 208602) and at the $(2.5, 5, 10) \times 10^{20} \text{ cm}^{-2}$ levels (black, highlighting nearby sources in the field), overlaid on a greyscale representation of the image. Panel (c) shows H I isovelocity contours from 985 km s^{-1} to 1210 km s^{-1} in intervals of 35 km s^{-1} , overlaid on a color representation of the velocity field image; the color bar is set to encompass the full velocity range of H I gas in the six detected sources. Panels (b) and (d) show the SDSS r-band image of the AGC 208602 field, displayed in a logarithmic stretch to highlight low surface brightness emission; the contours in (b) are the same as in panel (a), while the contours in (d) are the same as in panel (c). The six gas-bearing systems in the field are labeled, as is the early-type galaxy NGC3457. The H I beam size is $49''$, as shown in the bottom left of panel (a).

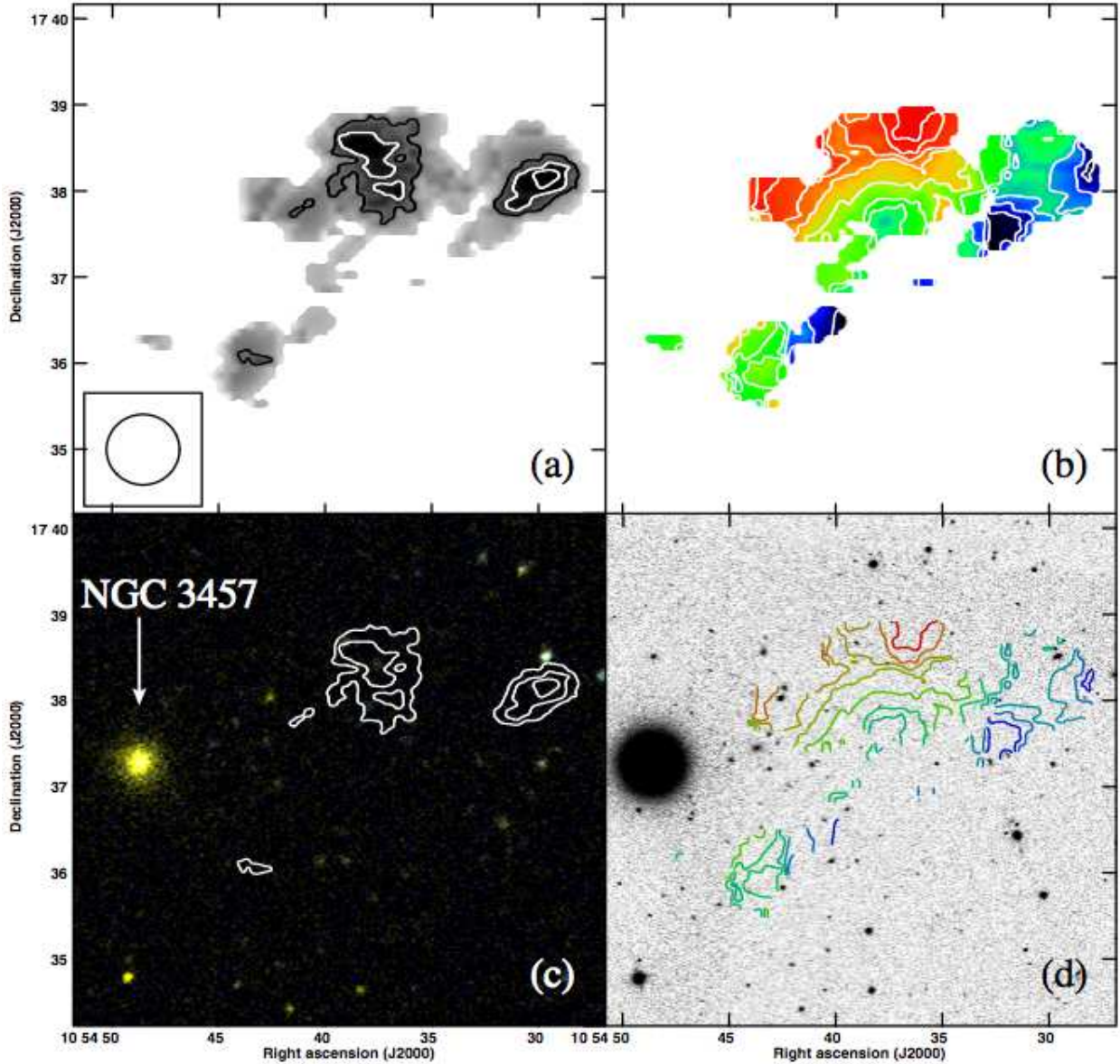


Fig. 5.— H I, SDSS R-band, and GALEX images of AGC 208602. Panel (a) shows H I column density contours at the $(0.35, 0.45, 0.55) \times 10^{20} \text{ cm}^{-2}$ levels, overlaid on a greyscale representation of the image. Panel (b) shows H I isovelocity contours from 1085 km s^{-1} to 1130 km s^{-1} in intervals of 5 km s^{-1} , overlaid on a color representation of the velocity field image. Panel (c) shows a color representation of the GALEX UV images, while panel (d) shows the SDSS r-band image (displayed in a logarithmic stretch to highlight low surface brightness emission); the contours in (c) are the same as in panel (a), while the contours in (d) are the same as in panel (b). The early-type galaxy NGC 3457 is labeled in panel (c); the systemic velocity of this galaxy ($V = 1148 \text{ km s}^{-1}$; Cappellari et al. 2011) suggests a physical association with the other galaxies in the AGC 208602 field. The velocity field was derived via a standard first moment analysis, using the same pixels that contribute to the column density (moment zero) image; the incoherent velocity structure of AGC 208602 precluded meaningful Gaussian fitting to the full data cube. The H I beam size is $49''$, as shown in panel (a).

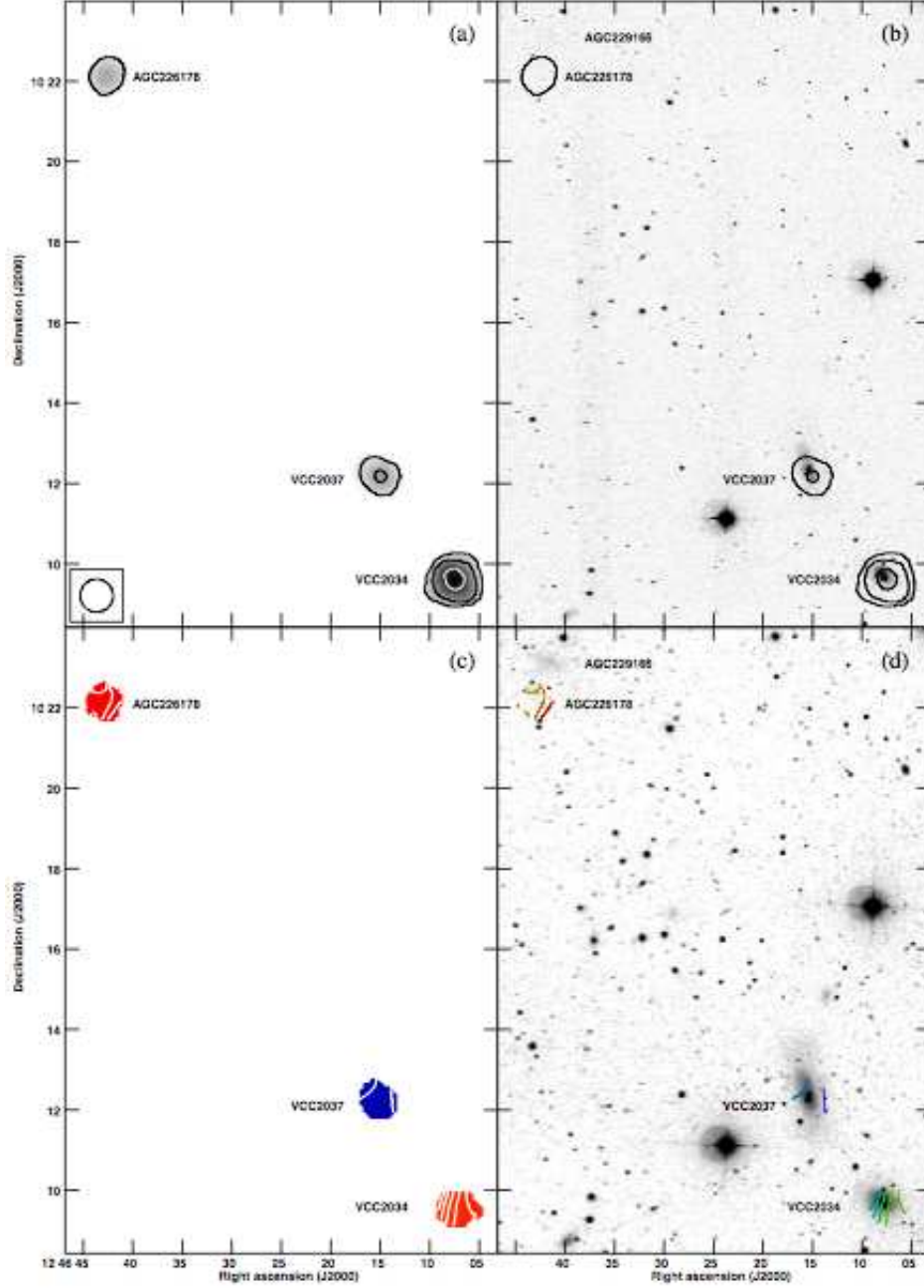


Fig. 6.— H I and SDSS R-band images of the AGC 226178 field. Panel (a) shows H I column density contours at the $(0.5, 1, 2) \times 10^{20} \text{ cm}^{-2}$ levels, overlaid on a greyscale representation of the image. Panel (c) shows H I isovelocity contours at the (1145, 1148, 1495, 1500, 1505, 1510, 1515, 1586, 1588, 1590) km s^{-1} levels overlaid on a color representation of the image; the color bar is set to encompass the full velocity range of H I gas in the three detected galaxies. Panels (b) and (d) show the SDSS r-band image of the AGC 226178 field; panel (b) is displayed in a logarithmic stretch to highlight low surface brightness emission, while panel (d) has been smoothed by a Gaussian kernel (see discussion in § 3.2). The contours in (b) are the same as in panel (a), while the contours in (d) are the same as in panel (c). The very low optical surface brightness source AGC 229166 is also labeled in panels (b) and (d). The H I beam size is $49''$, as shown in the bottom left of panel (a).

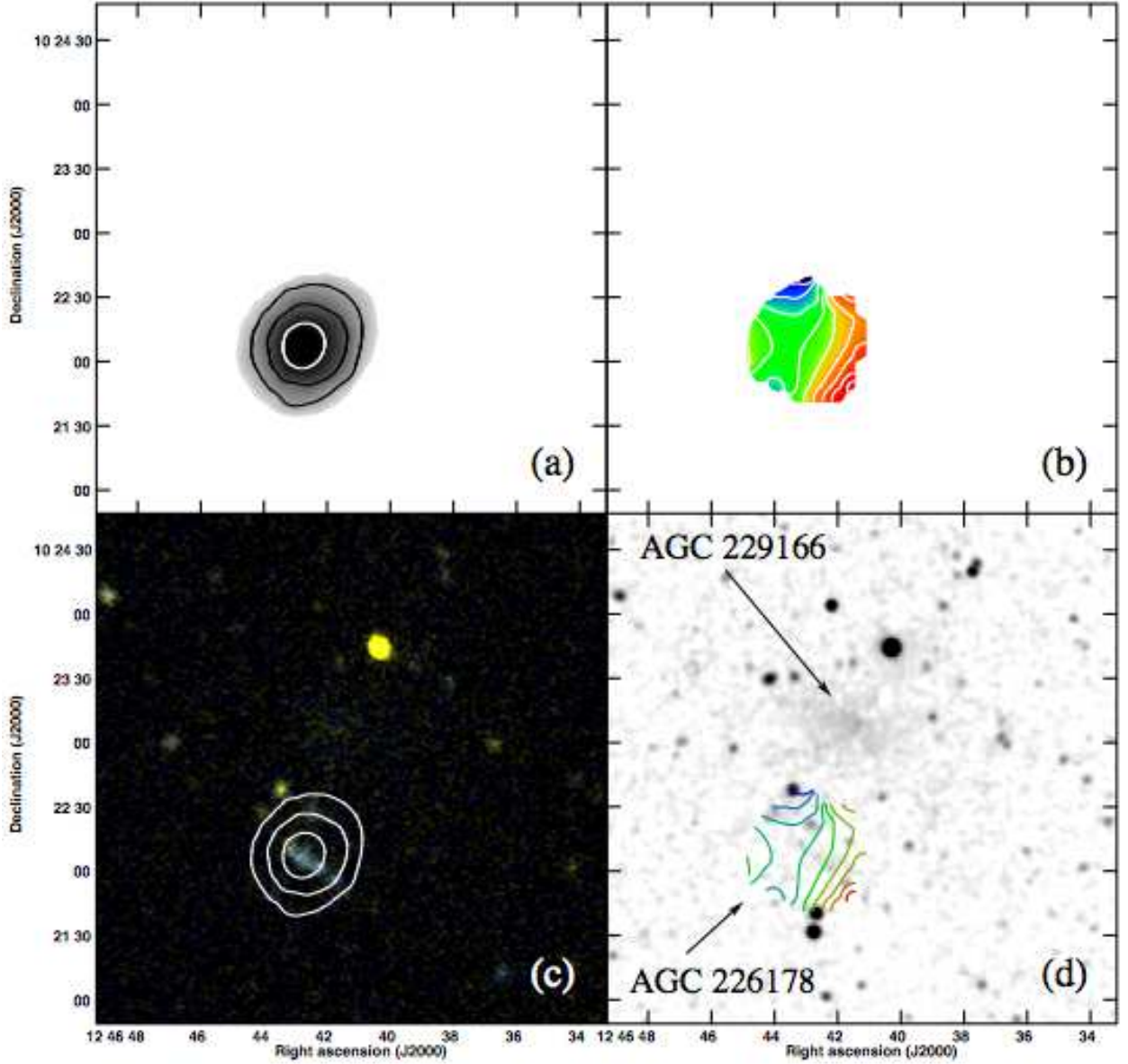


Fig. 7.— H I and SDSS R-band images of AGC 226178. Panel (a) shows H I column density contours at the $(0.5, 0.7, 0.9) \times 10^{20} \text{ cm}^{-2}$ levels, overlaid on a greyscale representation of the image. Panel (b) shows H I isovelocity contours from 1584 km s^{-1} to 1592 km s^{-1} in intervals of 1 km s^{-1} , overlaid on a color representation of the velocity field image. Panel (c) shows a color representation of the GALEX UV images, while panel (d) shows the SDSS r-band image (convolved by a Gaussian kernel to highlight low surface brightness emission); the contours in (c) are the same as in panel (a), while the contours in (d) are the same as in panel (b). The velocity field was derived by fitting Gaussian functions to the full data cube. The H I beam size is $49''$; the source is unresolved at this angular resolution.

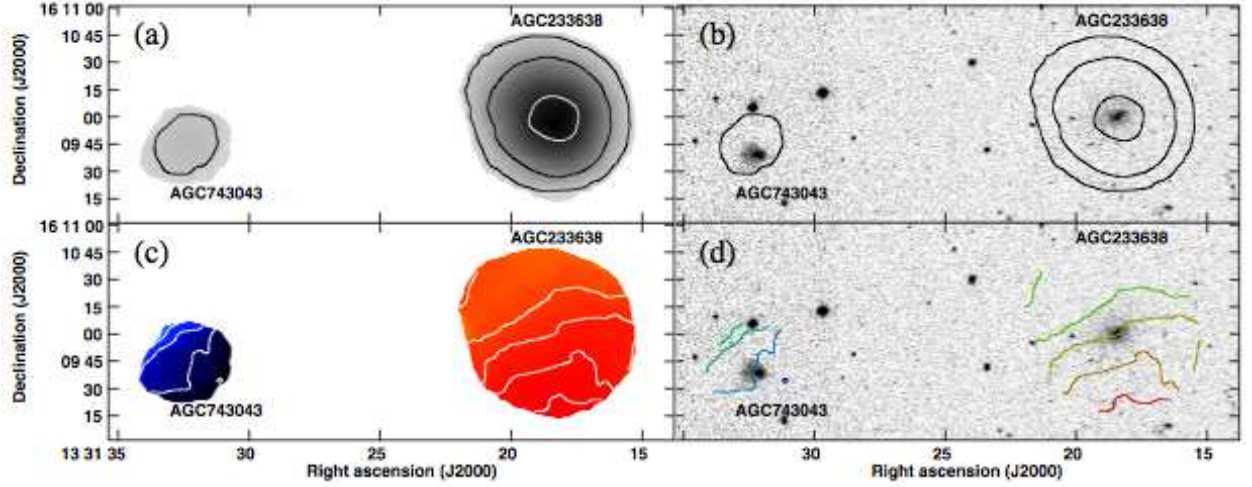


Fig. 8.— H I and SDSS R-band images of the AGC 233638 field. Panel (a) shows H I column density contours at the $(0.5, 1, 2) \times 10^{20} \text{ cm}^{-2}$ levels, overlaid on a greyscale representation of the image. Panel (c) shows H I isovelocity contours at the $(7330, 7335, 7340, 7345, 7400, 7405, 7410, 7415) \text{ km s}^{-1}$ levels overlaid on a color representation of the image; the color bar is set to encompass the full velocity range of H I gas in the two detected galaxies. Panels (b) and (d) show the SDSS r-band image of the AGC 226178 field, displayed in a logarithmic stretch to highlight low surface brightness emission; the contours in (b) are the same as in panel (a), while the contours in (d) are the same as in panel (c). The two systems in the field are labeled. The H I beam size is $60''$; at this angular resolution, AGC 743043 is unresolved, while AGC 233638 is marginally resolved.

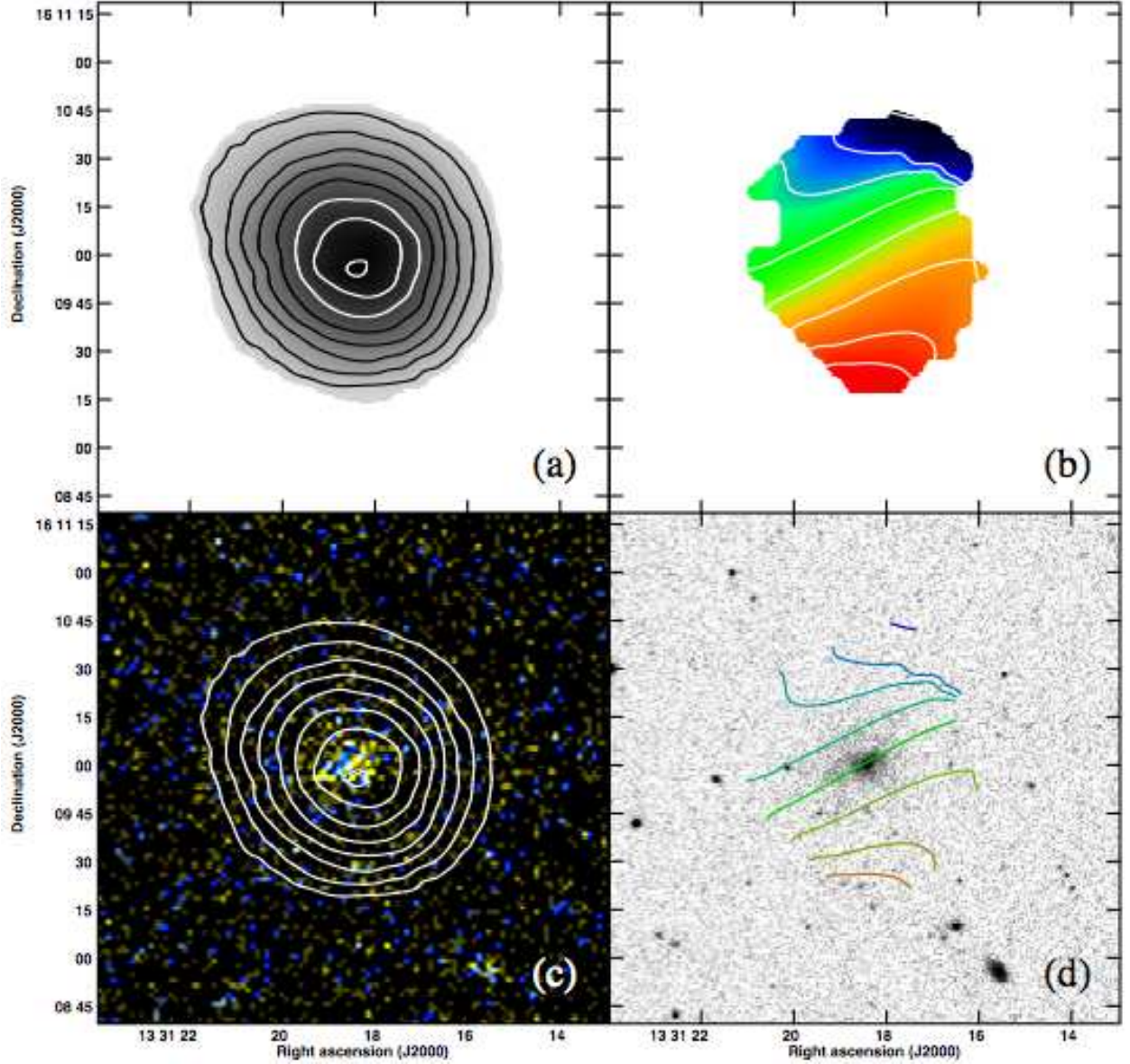


Fig. 9.— H I, SDSS R-band, and GALEX images of AGC 233638. Panel (a) shows H I column density contours at the $(0.5, 0.75, 1.0, 1.25, 1.5, 1.75, 2.0, 2.25) \times 10^{20} \text{ cm}^{-2}$ levels, overlaid on a greyscale representation of the image. Panel (b) shows H I isovelocity contours from 7385 km s^{-1} to 7420 km s^{-1} in intervals of 5 km s^{-1} , overlaid on a color representation of the velocity field image. Panel (c) shows a color representation of the GALEX UV images, while panel (d) shows the SDSS r-band image (displayed in a logarithmic stretch to highlight low surface brightness emission); the contours in (c) are the same as in panel (a), while the contours in (d) are the same as in panel (b). The velocity field was derived by fitting Gaussian functions to the full data cube. The H I beam size is $60''$; AGC 233638 is slightly resolved at this angular resolution.

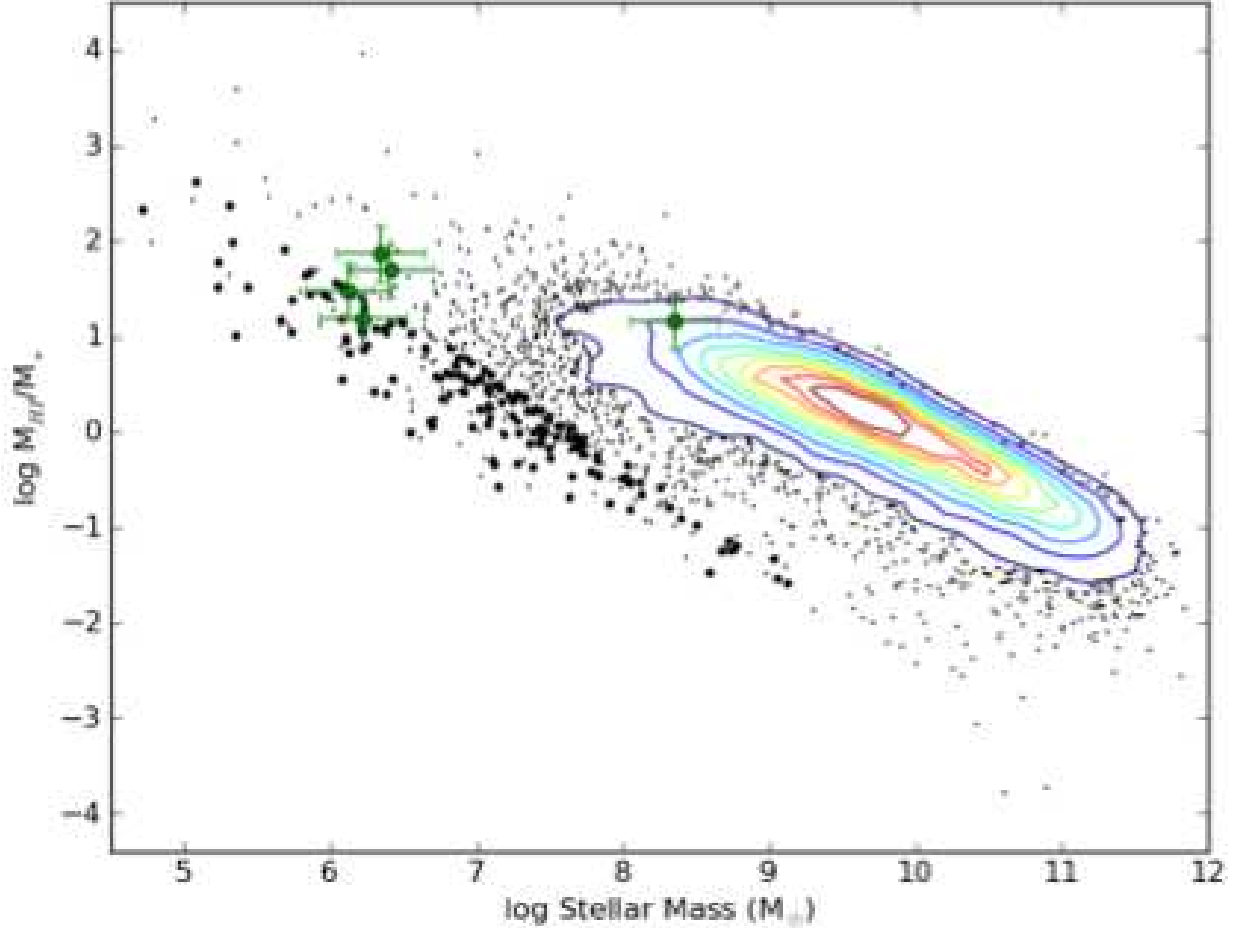


Fig. 10.— Plot of the logarithm of the neutral hydrogen to stellar mass ratio, M_{HI}/M_* , versus the logarithm of the stellar mass, for all members of the $\alpha.40$ catalog (Haynes et al. 2011). All small black points and areas within contours represent galaxies with reliable SDSS optical counterparts in the $\alpha.40$ catalog. The contours show number densities in intervals of 10%, from 10% to 90% of the number density maximum (which occurs at $\log(M_{\text{HI}}) = 9.8$; see Haynes et al. 2011). The dwarf galaxies from the Huang et al. (2012) sample are shown as thick black points; the five “Almost Dark” sources studied in this work are shown in green. With the exception of AGC 233638 (which may have contaminated photometry; see detailed discussion in § 1 and § 3.3.2), these objects preferentially populate the extreme upper left region of this plot.